

LAYER STRUCTURES FORMED BY SILICA NANOPARTICLES AND CELLULOSE NANOFIBRILS WITH CATIONIC POLYACRYLAMIDE (C-PAM) ON CELLULOSE SURFACE AND THEIR INFLUENCE ON INTERACTIONS

Jani Salmi,* Tiina Nypelö, Monika Österberg, and Janne Laine

A quartz crystal microbalance with dissipation monitoring (QCM-D) was used to study the adsorption of the layer formed by silica nanoparticles (SNP) and cellulose nanofibrils (NFC) together with cationic polyacrylamide (C-PAM) on cellulose surface, accompanied by use of atomic force microscope (AFM) to study the interactions between cellulose surfaces. The purpose was to understand the multilayer build-up compared to complex structure adsorption. The layer thickness and consequently also the repulsion between surfaces increased with each addition step during layer formation in the SNP-C-PAM systems, whereas the second addition of C-PAM decreased the repulsion in the case of NFC-C-PAM multilayer formation. An exceptionally high repulsion between surfaces was observed when nanofibrillar cellulose was added. This together with the extremely high dissipation values recorded with QCM-D indicated that nanofibrillar cellulose formed a loose and thick layer containing a lot of water. The multilayer systems formed fully and uniformly covered the surfaces. Silica nanoparticles were able to penetrate inside the loose C-PAM structure due to their small size. In contrast, NFC formed individual layers between C-PAM layers. The complex of C-PAM and SNP formed only a partly covered surface, leading to long-ranged pull-off force. This might explain the good flocculation properties reported for polyelectrolyte-nanoparticle systems.

Keywords: Adsorption; Surface force; Nanoparticle; Cellulose nanofibril; Polyelectrolyte; Multilayer; AFM; QCM-D

Contact information: Department of Forest Products Technology, Helsinki University of Technology, P.O. Box 3320, 02150 TKK, Espoo, Finland; *Corresponding author: jani.salmi@tkk.fi

INTRODUCTION

Charge based layer-by-layer deposition of polymer nanostructures was introduced in the 1990's. One of the pioneers was Decher (1992), who has reviewed the field of the early years in Science (1997). Polymer multilayers (PEM) were fabricated using alternating layers of oppositely charged polyelectrolytes. The method is based on charge reversal upon each adsorption step, which enables the adsorption in the next step and regulates the amount of adsorption. Polymers are typically flexible, and thus they form somewhat fuzzy nanostructures. This protects the layered structure from defects that are typical in crystalline films. Polyelectrolyte multilayering is a simple process, and in addition, it can be extended to colloids, nanoparticles, biomolecules, etc. Layer-by-layer assemblies of polyelectrolyte and nanoparticles were introduced by Kotov et al. (1995),

and for silica nanoparticles by Ariga and others (Ariga et al. 1997; Lvov et al. 1997). Lvov et al. (1997) studied the structure and the ordering of the silica-polyelectrolyte architecture on the silica surface and also compared layered structures to complexes. Multicomposites facilitate the combination of two or more desirable properties of the versatile polymers (Decher 1997). Even higher functionality can be achieved than the sum of the physical or chemical properties of the two separate components. The versatility of the nanostructures built in this way is remarkable (Lvov et al. 1997). Not only can the properties of polyelectrolytes be varied, but also the properties of nanoparticles (e.g. size) and the architecture of the nanostructure (different sequences, complexes). All these applications, however, require a good control of the organization at the nanoscale. The nanostructures can be used in new optics, biosensors, chemical catalysis, and biomedical applications (Decher 1997). Swelling of the polymer layers provides the possibility to use a polymer nanostructure as a drug carrier or a nanomachine.

The development of nanofibrillar cellulose has opened the possibility to use cellulose nanofibrils as part of molecular architectures (Pääkkö et al. 2007). Cellulose nanofibrils are obtained by the mechanical fibrillation of cellulose fibers or by bacterial activity. They are renewable, biodegradable, and strong, and they can form a swollen network in aqueous solution. Thus, there are great expectations for the use of cellulose nanofibrils (Berglund 2005; Hubbe et al. 2008; Zimmermann et al. 2008). This material could be used as a reinforcement agent in green-composites, as well as for manufacturing of nanopaper filters and membranes. In addition, nanofibrils can be used as building components of multilayers (Wågberg et al. 2008; Ahola et al. 2008a; Aulin et al. 2008). Wågberg et al. (2008) noticed that cellulose nanofibrils as a part of multilayers formed optically active films. This opens up the opportunity to use nanofibrils in electronics and sensors. Ahola et al. (2008a) noticed that cellulose nanofibrils have a positive effect on the wet and dry strength of paper. All in all, cellulose is a widely used material e.g. in paper, textile, and medical industries. Therefore, the study of the cellulose behavior with surface sensitive methods has a vast interest. A novel approach in this field is the use of nanofibrillar cellulose film as a representative model for the fibrillar outer surface of cellulosic fibers when investigating modifications and behavior of the cellulose surface.

Not only is the structure of layer-by-layer assemblies important, but also there is interest in their behavior in different circumstances and their influence on interactions. The structures formed by the polymers and nanoparticles play an important role in flocculation and stabilization in industrial scale processes, e.g. in sewage dewatering and in papermaking. The mechanism of flocculation depends upon the layer structure in common flocculation systems of a single polymer and a dual polymer and, hence, on the interactions in these systems (Salmi et al. 2007a and 2007b). As a continuation of those studies, nanoparticles can be introduced to the system. From the process point of view, microparticles and nanoparticles have been noticed to improve flocculation (Swerin and Ödberg 1996; Andersson and Lindgren 1996). The microparticle systems differ from the dual polymer systems in their better ability to reflocculate after floc breakage. The dual polymer system gives the largest degree of flocculation and the largest average floc size, while the microparticle system give a much smaller floc size at a comparable flocculation level (Wågberg and Lindström 1987). However, interactions on the molecular level in

nanoparticle-polyelectrolyte systems have rarely been studied (Sennerfors et al. 2000). To understand the structure of nanoparticle-polyelectrolyte assembly and the mechanism behind flocculation phenomena, we have studied the effect of silica particles upon adsorption on cellulose and on the interactions between cellulose surfaces during multilayer formation.

Despite the fact that the substrate surface has an influence on multilayer formation in the few first layers, most of the earlier studies have been made on mineral surfaces (Wågberg et al. 2008). The nanofibrillar cellulose (NFC) surface is a new material for the preparation of cellulose model surfaces and thus opens new possibilities to study adsorption and structures on a polymeric surface. The effect of silica nanoparticles, not to speak of nanofibrils, on surface interactions has been studied only to limited extent, and almost not at all on a cellulose surface. In this paper, the adsorption on nanofibrillar cellulose using quartz crystal microbalance with dissipation monitoring (QCM-D), and interactions between cellulose surfaces using atomic force microscope (AFM), were studied during multilayer formation of anionic silica nanoparticle and anionic cellulose nanofibrils with cationic polyacrylamide (C-PAM). Also the adsorption and the interactions of the complexes formed by the same components were investigated. The aim of this work is to clarify the properties of multilayers and complexes and to understand the effect of the formed nanostructure on interactions. In addition, the behavior of spherical inorganic nanoparticles is compared to the behavior of cellulose nanofibrils in the multilayer build-up. Results are also considered in the aspect of flocculation and web formation in papermaking, although these results can be extracted and generalized to other flocculation and stabilization phenomena in industrial processes.

EXPERIMENTAL

Materials

Low charge nanofibrillar cellulose (NFC) was used as a substrate in the QCM-D and AFM measurements. The cellulose nanofibrils were disintegrated from bleached sulphite pulp at STFI-packforsk, Stockholm, Sweden, using a high-pressure fluidizer (Microfluidizer M-110EH, Microfluidics Corp., Newton, MA) according to the procedure described by Pääkkö et al. (2007). In order to remove larger aggregates prior to film formation, the 2 % nanofibril gel was first diluted to 1.67 g/l and disintegrated with an ultrasonic microtip, a Branson Sonifier S-450 D (Danbury, USA) for 10 minutes with an amplitude of 25 %. The dispersion was then centrifuged with an Optima L-90K Beckman Coulter ultracentrifuge (USA) at approximately 8000 G (10 400 rpm) for 45 minutes. The charge of the low charge nanofibrils was about 44 $\mu\text{eg/g}$ (Pääkkö et al. 2007). Then the cellulose films were prepared by spin-coating the clear supernatant fluid of the nanofibrillar dispersion onto silica coated QCM-D crystals (Q-Sense AB, Sweden) or onto smooth silica wafers (Oktometic Oy, Finland), where 3-aminopropyltrimethoxysilane (APTS) was used as an anchoring substance (Ahola et al. 2008b). The spin-coated surfaces were rinsed with water, dried gently with nitrogen gas, and heat-treated in an oven at 80 °C for 10 min. This procedure leads into a film thickness of about 11 nm

(Ahola 2008) and into the crystallinity of cellulose I surface of about 70 % (Aulin et al. 2009).

In AFM force measurements, precipitated spheres of cellulose II regenerated via the viscose process (Kanebo Co., Japan) were used as colloidal probes. They were 5–35 % crystalline and slightly negatively charged (Carambassis and Rutland 1999). Their radius was 15–30 μm , as determined *in situ* in electrolyte solution by using an optical microscope and a digital camera. The lower surface was a NFC film on a silica wafer.

Cationic polyacrylamide, C-PAM, (Kemira Chemicals Oy, Finland) with molecular weight (M_w) of 1.4 million g/mol and charge density (CD) of 1.8 meq/g (17 mol-%) was used (Salmi et al. 2007a). C-PAM was ultra-filtrated with different cut-offs to narrow the M_w distribution. The inorganic silica nanoparticles had a surface area of 130 m^2/g and a particle size of 25 nm (Bindzil 40/130, Eka Chemicals, Sweden). They were negatively charged and had a charge density of 150 $\mu\text{eq}/\text{g}$ as determined by polyelectrolyte titration. They were used as received from the supplier. Cellulose nanofibrils with high charge density, received from STFI-packforsk, Stockholm, Sweden, were used for forming multilayers and complexes. The highly charged nanofibrils were prepared by performing a carboxymethylation pretreatment of the pulp (Wågberg et al. 2008). The dispersion was prepared similarly to the dispersion of low charged cellulose nanofibrils. The charge of the highly charged nanofibrils was 515 $\mu\text{eq}/\text{g}$ (Wågberg et al. 2008). Polymer solutions and nanoparticle dispersions were prepared using deionized water further purified with Millipore synergy UV equipment (Milli-Q, Millipore S.A.S, Molsheim, France). A solution of 1 mM NaHCO_3 was used to buffer the pH in all solutions. The electrolyte concentration was adjusted using analytical grade NaCl.

Solution Properties

Measurements with AFM and QCM-D were performed in solutions of cationic polyacrylamide, silica nanoparticles, or highly charged nanofibrillar cellulose, as well as their complexes. In layer forming, the concentration of the single component solutions was 100 mg/l. The surface was rinsed with water between steps during multilayer formation. C-PAM solutions were diluted from a 2 g/l stock solution. The complexes were prepared by adding the C-PAM stock solution to abundant water, followed by the NFC or by the silica nanoparticle solution. The complex concentration was varied from 0 to 100 mg/l in force measurements. The complexes were mixed in mass ratios of 9:1 and 1:1 (C-PAM : nanoparticle), but the results did not deviated between the ratios, hence, only the ratio of 1:1 is presented in results. In all measurements, fresh solutions were prepared prior to use.

The average diameter of the complexes was determined by dynamic light scattering using a N5 Submicron Particle Size Analyzer (Beckman Coulter Inc., USA) in 50 mM NaHCO_3 . The zeta potentials of the complexes were determined using a Coulter Delsa 440SX Electrophoretic Light scattering Analyzer (Coulter Electronics Ltd., UK) at 5 V with a run time of 120 s with solutions in 1 mM NaHCO_3 . The properties of the complexes are presented in Table 1. The solution containing NFC and C-PAM was unstable and very sensitive to the preparation procedure. The cellulose fibrils were easily flocculated in the dispersion.

Table 1. Properties of the Complexes.

Complex	Mass ratio	Diam. / nm	Zeta-pot. / mV
C-PAM + SNP	9:1	360	-23
C-PAM + SNP	1:1	420	-16
C-PAM + NFC	9:1	260	-24
C-PAM + NFC	1:1	not stable	-26

SNP = silica nanoparticle, NFC = nanofibrillar cellulose

QCM-D Adsorption Measurements

The adsorption of complexes and multilayer structures on cellulose was studied using a quartz crystal microbalance with dissipation monitoring (QCM-D). The E-4 instrument was supplied by Q-sense AB (Västra Frölunda, Sweden). The QCM-D measures change in frequency and dissipation simultaneously at the fundamental resonance frequency, 5 MHz, and its overtones 15, 25, 35, 45, 55, and 75 MHz. The third overtone (15 MHz) of the QCM-D measurements was used for interpreting the adsorption results. Adsorption experiments were done on cellulose nanofibril model surfaces. Prior to the adsorption experiments, the NFC model surfaces were allowed to swell overnight in the buffer solution of 1mM NaHCO₃ or in 1 mM NaHCO₃ / 10 mM NaCl. The measurements were started by flowing the buffer solution through the chambers for at least 30 minutes to reach a horizontal baseline. After adsorption of the complexes and between each layer in multilayer build-up, the system was also rinsed with the buffer. Each experiment was repeated at least twice. The concentration of C-PAM, nanoparticle and the complex solutions was 100 mg/l.

AFM Imaging

To characterize the coverage, morphology, and roughness of the formed structures, the samples were imaged after the force measurements using an atomic force microscope, AFM (Nanoscope IIIa multimode scanning probe microscope, Digital Instruments Inc., Santa Barbara, USA). The AFM images were scanned in tapping mode in air using silicon cantilevers (NSC15/AIBS) delivered by MicroMasch, Estonia. The drive frequency of the cantilever was 310-350 kHz. The size of the images was 1 µm or 5 µm, and images were recorded on at least seven different areas of the two samples. No image processing except flattening was made. The imaging was performed at 30–40% relative humidity at 25 °C. A Scanning Probe Image Processor (SPIP, Image Metrology, Denmark) was used to analyze RMS roughness (ISO standard 4287/1), and to perform grain analysis of the surface features.

AFM Force Measurements

AFM was also used to measure surface forces between a cellulose sphere and a low charged nanofibrillar cellulose surface using the colloidal probe technique (Butt 1991; Ducker et al. 1991). A cellulose sphere was glued to the tipless end of the AFM cantilever with a reported spring constant of 0.06 N/m (Veeco Instruments, USA). Prior to measurements, the surfaces were allowed to equilibrate in the respective electrolyte

solution overnight. When changing the solution, the system was allowed to stabilize for 1 h. This procedure has been found to provide reliable and reproducible results (Paananen et al. 2004). The spring constants of the cantilevers were determined by the thermal noise method, and the result was controlled by the reference spring method (Hutter and Bechhöfer 1993; Torii et al. 1996; Tortonese and Kirk 1997). For the sake of clarity, only one representative curve per system is shown in the figures.

The raw data (cantilever deflection vs. piezo movement) were converted into force curves (force vs. separation) using the SPIP and were further manipulated in Origin (OriginLab Co., USA) (Salmi et al. 2007a). To facilitate a comparison to other studies, the forces in this study were normalized to the radius of the cellulose sphere used as the upper surface (Derjaguin 1934). The results were fitted to the interactions predicted by the DLVO theory of colloidal stability using the linearized Poisson-Boltzmann equation for constant charge and constant potential (Derjaguin et al. 1987). In the van der Waals part of the DLVO theory, the Hamaker constant of 0.8×10^{-20} J was used for cellulose in water (Bergström et al. 1999). The hydrodynamic forces were not included in the predictions, but measures were taken to minimize their influence on the experimental results. Thus, the approach velocity of the cellulose beads to each other was kept fairly low. The typical approach velocity was between 100 and 500 nm/s. We did not observe any effect of velocity on the interactions at the two approach velocities used, and 200 nm/s has previously been reported to be sufficiently low for the hydrodynamic forces between cellulose surfaces to be negligible (Stiernstedt et al. 2006). However, nanofibrillar cellulose tended to form a gel-like layer, and thus we cannot rule out the dynamic effect due to an increase in viscosity near the surface in the case where NFC was in solution, although no such effect was observed.

A clear constant compliance region could not be reached for the all systems due to compressibility of the layers. This may lead to erroneous result, if it is not taken into account (Rutland et al. 2004). In these cases, raw data (deflection versus piezo movement) was transferred to force curves by using the sensitivity value obtained for cellulose-cellulose contact. For the cellulose–cellulose contact, a constant compliance regime was attained due to the low spring constant of the cantilevers used in the experiments. The compressibility (load/indentation, $\mu\text{N}/\text{m}$) of such surfaces was analyzed from the force curve.

RESULTS

QCM-D Adsorption

Adsorption of C-PAM/nanoparticle and C-PAM/nanofibril multilayers on cellulose

The build-up of multilayers formed from either C-PAM and SNP or from C-PAM and high charged NFC was performed in low (1 mM) and medium (11 mM) salt concentrations. In Fig. 1, the change in frequency (Δf) and the change in dissipation (ΔD) as a function of time is shown at medium electrolyte concentration.

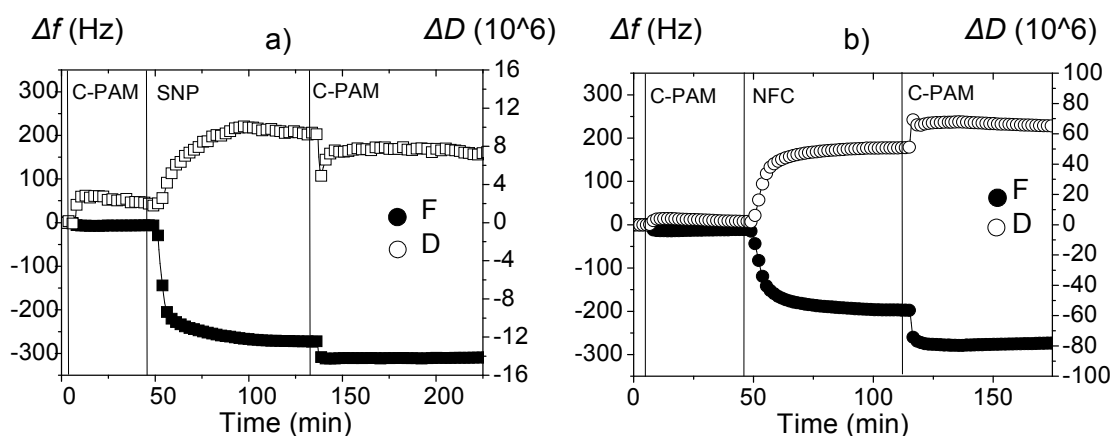


Fig. 1. Change in frequency (filled marks) and dissipation (open marks) upon adsorption of multilayers of a) C-PAM and SNP and b) C-PAM and NFC on cellulose in 11 mM electrolyte concentration (medium salt). After each layer the system was rinsed with the buffer solution. The 3rd overtone was used in the graphs. Note that different scales were used for dissipation values.

Adsorption of both C-PAM and nanoparticles was observed as a decrease in Δf . However, a clearly larger decrease in frequency was observed upon adsorption of nanoparticles (SNP and NFC) than upon adsorption of C-PAM. The layer properties of the two nanoparticle systems were totally different, as indicated by the different responses in dissipation during adsorption. Adsorption of SNP on C-PAM resulted in a small increase in dissipation, but relatively large change in frequency. One reason for this could be that the SNPs were immersed inside the C-PAM layer. A rather high amount of nanoparticles could be added. When C-PAM was added the second time, the frequency change slightly increased, but the dissipation decreased, implying that the layer was getting denser (Fig. 1a and 2b).

When NFC was adsorbed on C-PAM, the change in frequency was slightly less, but the trend was similar to the SNP case ($\Delta f = 186$ Hz vs. 266 Hz, respectively). However, the dissipation increased greatly ($\Delta D = 48$ vs. 8, respectively). Similar behavior in the case of NFC has been seen earlier by Ahola et al. (2008b). This behavior is most probably due to the very high water binding capacity of cellulose nanofibrils. Nanofibrils adsorbed on C-PAM are strongly bound, and the layers are retained well despite rinsing after each addition.

Clearly, the adsorption of C-PAM was faster than the adsorption of nanofibrils. This can be explained by comparing the structure of the two very different substances. NFC is a fibrous material having lengths in the micrometer scale, while C-PAM has an average R_g of approximately 300–400 nm (Mabire et al. 1984). C-PAM is flexible and small compared to the cellulose nanofibrils; therefore, the conformational changes are faster with C-PAM, leading to faster adsorption. Furthermore, the binding of water affects the adsorption behavior of NFC and its ability to form a network.

In Fig. 2, the maximum change in frequency and dissipation for each layer is compared in medium and low salt concentrations for the two systems. Although only four layers were adsorbed, it is clear that layer growth was not linear. The change in frequency after the second nanoparticle addition was clearly higher than for the first addition. In the

case of the SNP system, a high final frequency change was reached after four layers, while dissipation change stayed low at both salt concentrations. In the case of the NFC multilayer system, the dissipation increased relative to the increase in the frequency change when salt concentration was increased (Fig. 2). A slight drop in dissipation could be detected in the NFC system at low salt concentration upon adsorption of a second C-PAM layer. This implies that the NFC layer collapsed due to the penetration of C-PAM molecules into the loose NFC layer. As already seen in Fig. 1, a similar drop took place also in the SNP system; however, the effect was present in both salt concentrations. It has previously been observed that addition of some electrolyte (10mM) is beneficial for multilayer formation (Aulin et al. 2008). This observation correlates well with these results.

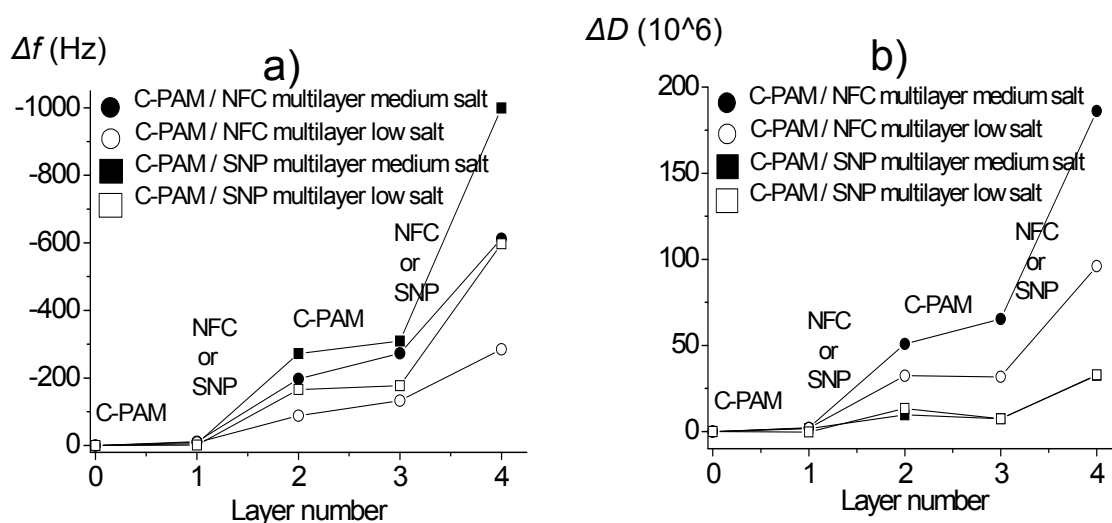


Fig. 2. The effect of the salt concentration, 1 mM or 11 mM electrolyte concentration (low salt or medium salt, respectively), on a) frequency and b) dissipation of NFC/C-PAM and SNP/C-PAM multilayer adsorption (3rd overtone) on cellulose. The values were taken after adsorption and rinsing of each layer.

The measurement data of the 5th and 7th overtones is not presented here. However, scattering between the 3rd, 5th and 7th overtones in the NFC multilayer system indicates that the adsorbed mass was dependent on frequency. This implies that the layer was not homogeneous in depth. The bound water in NFC can cause the difference in properties inside the layer. This behavior was not observed in the SNP multilayer system, for which all overtones gave similar results.

Adsorption of C-PAM/nanoparticle and C-PAM/nanofibril complexes on cellulose

The adsorption of preformed complexes of C-PAM and either SNP or NFC revealed different adsorption characteristics between the systems. The rate of adsorption of C-PAM/SNP complexes was fast, whereas no plateau was reached during the adsorption of C-PAM/NFC complex before rinsing (Fig. 3). Similar conformation changes for complexes made of NFC and poly(amidamine) epichlorohydrin (PAE) have been noted by Ahola et al. (2008a).

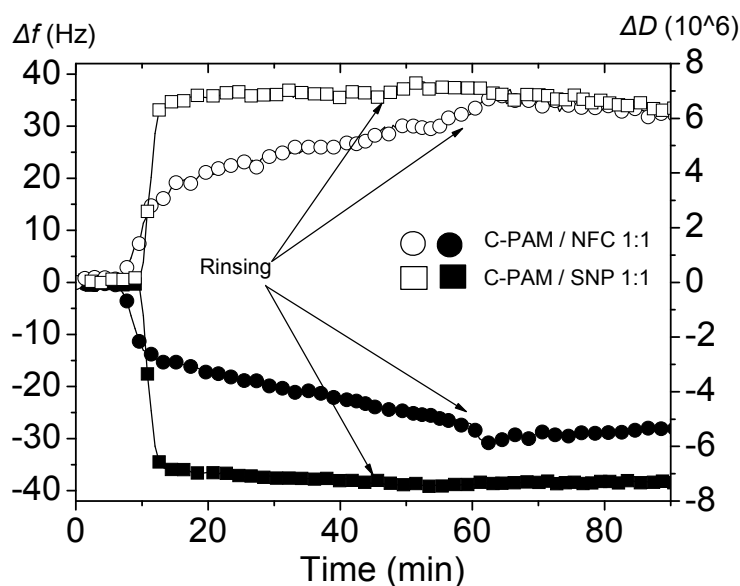


Fig. 3. Frequency (filled marks) and dissipation (open marks) changes of 3rd overtone upon adsorption of C-PAM/SNP (square marks) and C-PAM/NFC (spherical marks) complex structures on cellulose from 11 mM electrolyte concentration (medium salt) with weight ratio of 1:1.

The difference in the adsorption kinetics between SNP and NFC complex systems seen in Fig. 3 can also be inferred from the frequency vs. dissipation plots. With two minutes between consecutive datapoints, the Δf vs. ΔD plots of the two systems in medium and in low salt concentrations are shown in Fig. 4. Crowding of the SNP data points reveals the quick balancing of the adsorption, whereas the continuous adsorption of NFC systems is seen as a steady increase in both dissipation and frequency.

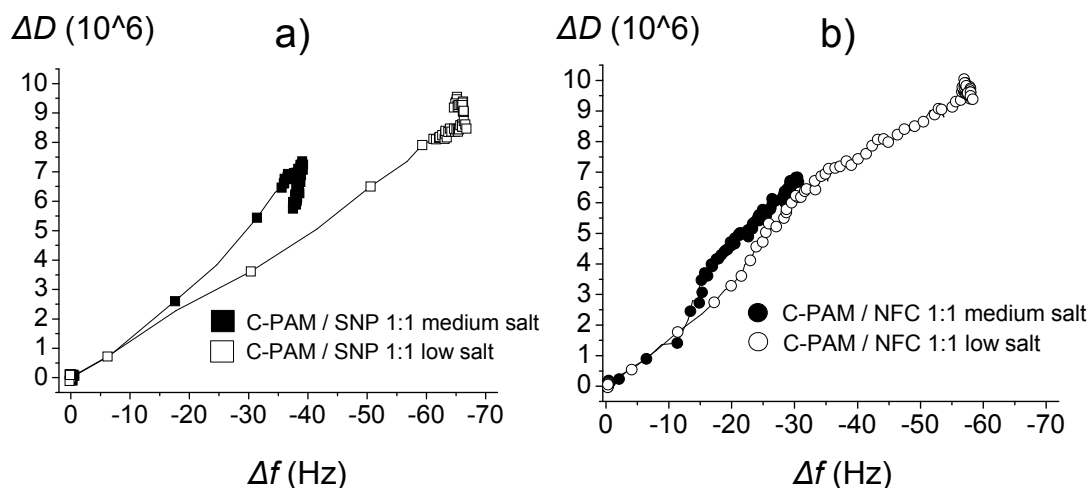


Fig. 4. Relation between frequency and dissipation values of a) C-PAM/SNP and b) C-PAM/NFC complexes in 1mM and 11 mM electrolyte concentration (low salt or medium salt concentration, respectively).

An increase in the electrolyte concentration resulted in a looser layer structure (higher change in dissipation versus change in frequency, i.e. a larger slope in curve) for the SNP/C-PAM complex. In case of NFC/C-PAM complex this effect was not as clear. In Fig. 5, a bilayer of C-PAM/nanoparticles is compared to the corresponding complex. Clearly, a much thicker layer was reached using multilayering. This behavior is different from earlier observations using the polyelectrolyte complexes (Saarinen et al. 2008). However this can also be affected by the fact that each solution adsorbed in multilayering had a concentration of 100 mg/l, whereas the total concentration of a complex was also 100 mg/l.

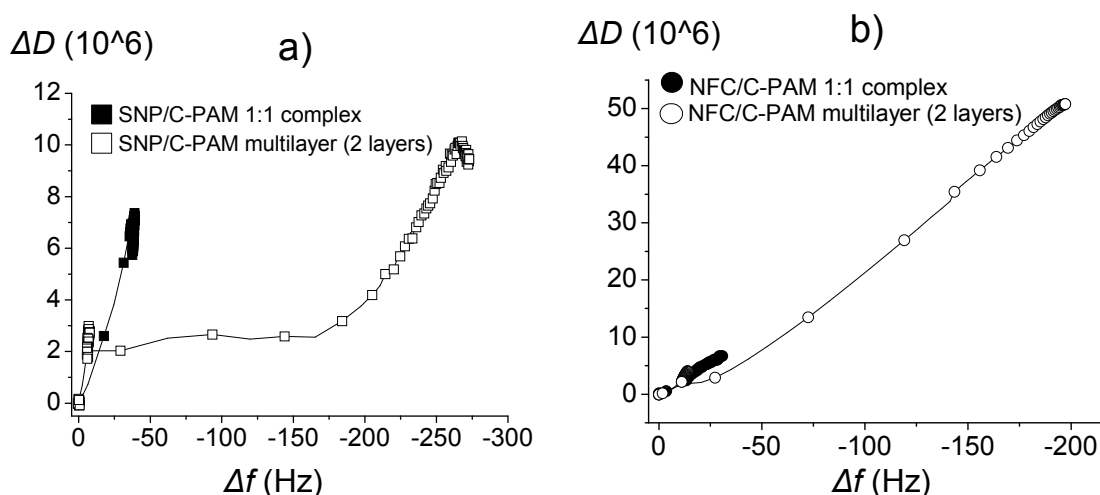


Fig. 5. Relation between frequency and dissipation values of the multilayer and the complex systems of a) C-PAM/SNP and b) C-PAM/NFC complexes in 11 mM electrolyte (medium salt) concentration .

AFM Imaging of the Multilayer and Complex Systems

The effect of the different adsorption strategies on the topography of the adsorbed film is compared in Fig. 6. The image of the pure nanofibrillar cellulose surface (Fig. 6a) was recorded before the measurements. The RMS roughness was measured to be 3.5 nm. The other samples were rinsed with water after adsorption and dried before imaging in air. The structure of the nanofibrillar cellulose surface clearly changed during multilayer formation in the silica system. After the C-PAM – SNP – C-PAM adsorption cycle, a layer of clusters covered the whole sample when the adsorption was performed in medium salt concentration (Fig. 6b). Similar ordering has been observed earlier (Lvov et al. 1997; Bogdanovic et al. 2002). The size of the clusters was roughly 180 x 60 nm. At higher magnification it was observed that the clusters were formed from a few smaller granules. The approximate size of a single granule was 80 x 40 nm. The height of the granules could not be determined, because the granules were aligned too closely to one other. The RMS roughness determined from 5 x 5 μm images was 24 nm.

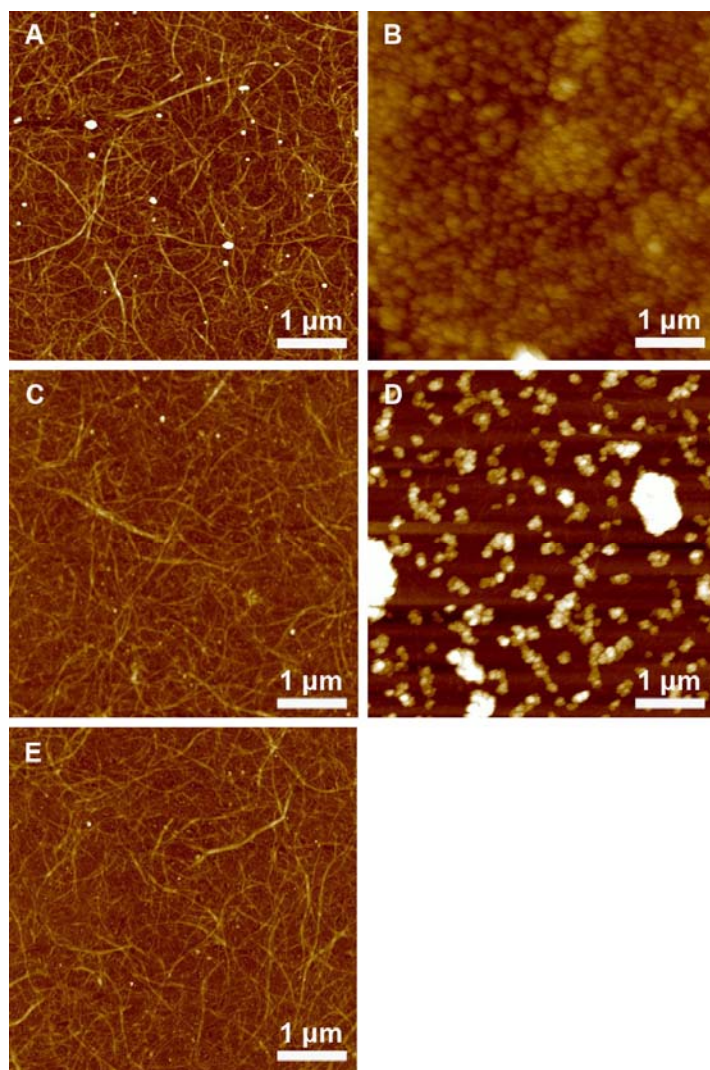


Fig. 6. AFM height images: A. A NFC surface before any measurement. B. The layer structure of C-PAM – SNP – C-PAM. C. The layer structure of C-PAM – NFC – C-PAM. D. The complex structure (at mass ratio of 1:1) of SNP and C-PAM. E. The complex structure of NFC and C-PAM. The sizes of images are 5x5 μm and height scales are a. 40 nm, b. 400 nm, c. 50 nm, d. 150 nm, and e. 50 nm. Samples from b to e were prepared in 11 mM electrolyte concentration, then rinsed and dried after force measurements.

The multilayer of C-PAM and highly charged NFC showed a nanofibrillar structure in the AFM image with an RMS roughness of 2.6 nm (Fig. 6c). The topographical structure was very similar to the unmodified NFC surface (Fig. 6a). The RMS roughness of the layered structure was only slightly lower than in the low charged nanofibrillar cellulose surface (3.5 nm). In addition, it was well within agreement with the value of 2 nm reported by Ahola et al. (2008b) for highly charged nanofibril films made by spin coating. The QCM-D data showed that adsorption had occurred, and that the formation of layers was continuous. Hence, it was concluded that this surface was covered and that the NFC was evenly distributed over the whole sample.

AFM imaging of the samples of C-PAM-silica nanoparticle complexes (mass ratio of 1:1) revealed that the substrate was not fully covered by the nanoparticles. The structure of the nanofibrillar cellulose was clearly seen beneath clusters on sample prepared at medium salt concentrations (Fig. 6d). Clusters were 140-300 nm in length and 45-100 nm in width. Furthermore, the clusters seemed to be formed by smaller granules. Overall, the size of the clusters as well as the size of single grains was comparable to observation on the multilayer surfaces. The height of the single grains was 25-40 nm, which is very close to the reported size of SNP (25 nm). The values of RMS roughness for the complex samples were 17 nm, which was caused by the surface being only partly covered.

It is impossible to say whether the complex of C-PAM and NFC was adsorbed or not on the surface based on the AFM images (Fig. 6e). They looked identical to the substrate (Fig. 6a). The RMS roughness was a comparable 2.8 nm. However, we found that NFC and C-PAM formed rather large aggregates, and the amount of their adsorption was low. Hence, it is probable that the complex was removed during rinsing.

The effect of salt concentration on the parameters determined from the AFM images is shown in the Table 2. The effect of salt concentration was minor. The only notable difference was that the C-PAM-SNP clusters were slightly smaller at low salt. However, the adsorption of the complexes observed with QCM-D was seen to be higher at low salt. This deviation may be due to the areal variation of imaging sample or more probably to the fact that AFM images were recorded for dry samples. On the other hand, change in frequency in QCM-D is very much affected by bound water in the complex.

Table 2. Topographical Properties of AFM Images

	Multilayer			Complex		
	SNP-C-PAM		NFC-CPAM	SNP-C-PAM		NFC-CPAM
c_s (mM)	1	11	11	1	11	11
Coverage (%)	100	100	100	10-20	15-30	Uncertain
Size of cluster (nm)	120x45	180x60	-	125x40	220x70	-
Z mean range (nm)	6	10	-	19	18	-
RMS (nm)	8	24	2.6	15	17	2.8

Surface Forces between Cellulose Surfaces

The surface forces were measured during the layer formation using AFM. The interactions between a cellulose colloidal probe and the nanofibrillar cellulose surface during the build-up of the layers were followed in 1 mM and 11 mM electrolyte concentration. During stepwise addition the concentration of solution was 100 mg/l, while the complexes were studied as a function of the concentration.

The influence of multilayer structure formed by C-PAM and SNP

The normalized surface forces during C-PAM – SNP – C-PAM layer formation are presented as a function of separation in Fig. 7. The interactions between the pure cellulose surfaces before polyelectrolyte addition were repulsive. This is congruent with

our earlier observations on the interactions between a NFC surface and cellulose sphere (Ahola et al. 2008b). Repulsion increased with each adsorbed layer. Cationic C-PAM adsorbed onto the negatively charged cellulose and led to charge reversal, as observed earlier (Salmi et al. 2007a). Further, negatively charged nanoparticles adsorbed on the C-PAM layer, increasing repulsion only slightly at low salt concentration (Fig. 7a). However, the addition of silica nanoparticles caused a clear increase in repulsion at medium salt concentration (Fig. 7b). This indicates a different layer structure. Again, C-PAM adsorbed on the C-PAM – SNP layer, which is assumed neutral or negatively charged, at both salt concentrations increased repulsion. The effect of SNP on the interactions agrees with results reported by Sennerfors et al. (2000). Repulsion in any solution did not follow the DLVO theory (Derjaguin et al. 1987). Thus, the repulsion was concluded to be mainly of steric origin. The overlapping of opposing layers between the approaching surfaces resulted in steric repulsion between the surfaces. Evidently, the layers became thicker while multilayer formation progressed, as is seen from the QCM-D data. At low salt concentration, the range of repulsion was longer than at medium salt concentration, due to electrostatic repulsion between similar charges in the layer causing a thicker structure.

Surface forces upon retraction, i.e. pull-off forces, were recorded together with the approaching data at both salt concentrations. Pull-off force between unmodified cellulose surfaces was small, as has been observed earlier (Holmberg et al. 1997b; Carambassis and Rutland 1999; Zauscher and Klingenberg 2000; Ahola et al. 2008b). Pull-off force disappeared or remained low during layer formation. This suggests that C-PAM – SNP layers do not mix or entangle during contact. Also, the compressibility (load /indentation) was analyzed from the force curves. Surface compressibility decreased in the build-up of the trilayer at low salt concentration, i.e. the surface became more easily compressible. This supports the thickening of the layer structure. Surface compressibility, however, did not decrease until second C-PAM addition at medium salt concentration. Then it decreased to the same level as the values observed at low salt concentration.

The influence of multilayer structure formed by C-PAM and highly charged NFC

In order to evaluate the effect of nanoparticle type on interactions, surface forces were studied also in the adsorption of the cellulose nanofibrils with C-PAM. These results were compared to interactions of the inorganic silica nanoparticle adsorption. Size, shape and chemistry were totally different in these two cases. In Fig. 8, the normalized surface force between cellulose sphere and low charged nanofibrillar cellulose surface are presented as a function of the relative separation during layer formation of high molecular weight C-PAM and highly charged cellulose nanofibrils. Clear differences between nanoparticle systems were observed. Repulsion increased substantially when highly charged nanofibrils were added into solution after the first C-PAM step. The range of the surface force was even over 1500 nm. Interestingly, repulsion decreased clearly when C-PAM was added the second time. This indicates that the adsorption of C-PAM collapsed the layer of high charged nanofibrillar cellulose. Surface forces during layer build-up did not follow DLVO theory, and thus it may be concluded that the interactions were mainly influenced by steric forces.

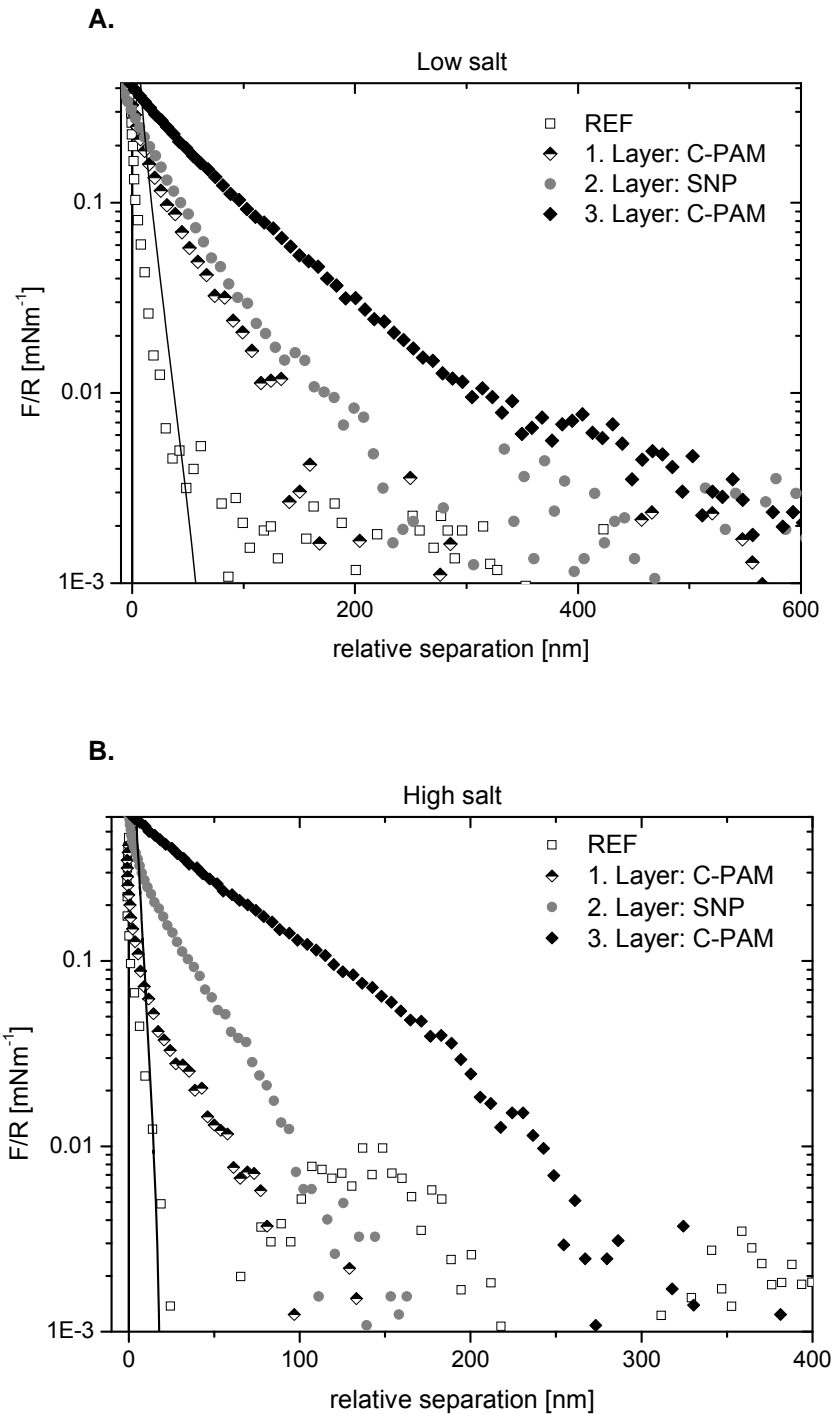


Fig. 7. Surface forces between a low charged cellulose nanofibril film and a cellulose sphere measured during the formation of the layer structure C-PAM – SNP – C-PAM at A. 1 mM electrolyte concentration and B. at 11 mM electrolyte concentration. The solid line shows the expected decay length of DLVO forces at the respective electrolyte concentration.

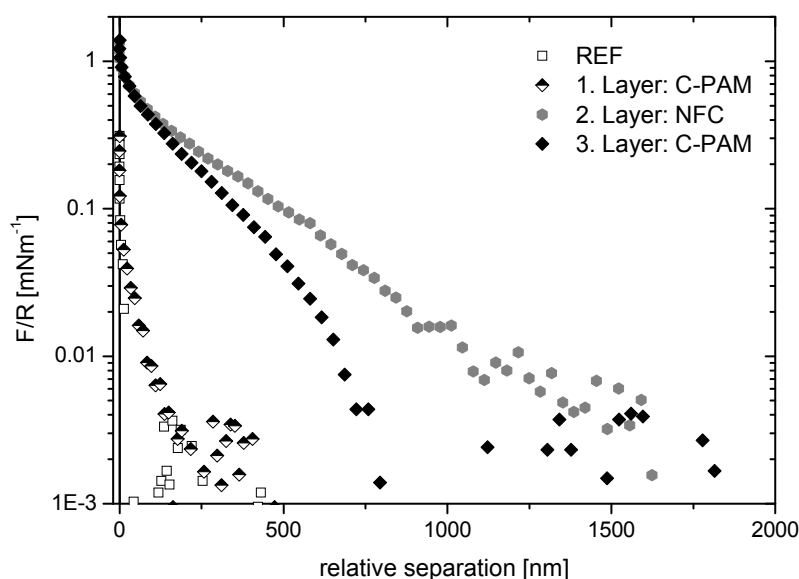


Fig. 8. Surface forces between cellulose surfaces measured in the formation of the trilayer structure C-PAM – highly charged NFC – C-PAM at 11 mM electrolyte concentration. In each step the concentration was 100 mg/l of C-PAM or NFC.

As in C-PAM-SNP layer formation, pull-off force disappeared during layer formation in the nanofibrillar cellulose system. In addition, compressibility of the layered surfaces decreased slightly, but not as much as in the silica nanoparticle case. Furthermore, compressibility increased slightly after the second addition of C-PAM. This supports the observation about the collapse of the layer. The measurement with highly charged cellulose nanofibrils was complicated due to system instabilities. It was quite common that the baseline of force curve was gradually tilting when the probe was approaching the surface. This was caused by the AFM probe being captured by a net of nanofibrils. For the same reasons, measurements with the C-PAM-NFC complex could not be performed.

The influence of C-PAM - SNP complexes

When C-PAM and silica nanoparticles were added together in a mass ratio 1:1, interactions between the cellulose sphere and nanofibrillar cellulose were recorded as a function of polymer-nanoparticle and NaCl concentration (Fig. 9). At both salt concentrations, repulsion increased when the concentration of the premixed complex increased from 0 mg/l to 100 mg/l. However, it was observed that the force upon approach, the pull-off force, and compressibility were dependent on location where the measurement was done. In Fig. 9, only the maximum effect is shown. The dependence on location was expected, when considering the partial coverage of the surface revealed by AFM (Fig. 6d). The interaction between the partly covered cellulose surfaces did not follow DLVO forces, indicating steric repulsion. The effect of salt concentration was also monitored. At medium salt concentration, the range of repulsion was slightly shorter.

This is most probably due to the decrease in electrostatic repulsion inside the complex, which decreases the steric repulsion, but may partly be due to the location variation of the incompletely covered surfaces. Further, QCM-D results and AFM images indicated that the amount of water in the complex layer was higher at low salt. Thus, complexes were larger at low salt concentration, resulting in longer repulsion as predicted by Donnan theory (Donnan 1912; Procter and Wilson 1916).

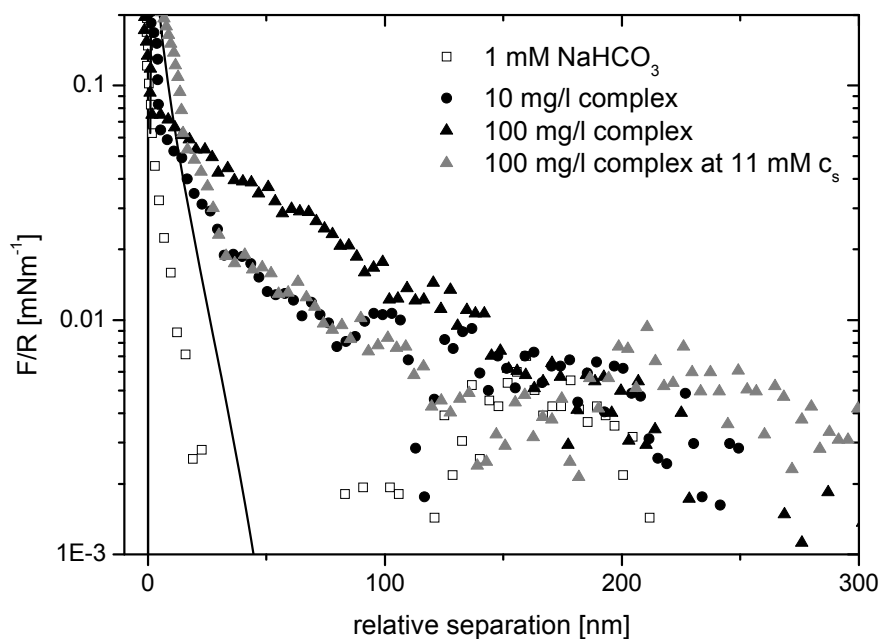


Fig. 9. Surface forces under the influence of C-PAM and silica nanoparticle complexes (mass ratio 1:1). Filled symbols are measurements done in 1 mM NaHCO₃ and open symbols are measurement done in 11 mM electrolyte (medium salt) concentration. The solid line represents the fitting of DLVO forces with constant charge.

Surface interactions with the complex structures differed clearly from the stratified structures in the matter of pull-off force (Fig. 10). The range and magnitude of pull-off force between complex layers increased when complex concentration increased, agreeing well with Sennerfors et al. (2000). Logically, the pull-off force originates from the partial coverage. Complexes are able to attach to both surfaces when the surfaces were pressed together. When the surfaces are withdrawn, the complexes stretch and detach slowly from the surface. It was noted that the range and magnitude of pull-off force was related with repulsion and compressibility. When repulsion was stronger, also the pull-off force was stronger and longer, while compressibility was lower. In other words, when more complexes were in the measuring area, stronger repulsion was observed and more complexes were able to form more bonds between surfaces, and thus produce a longer and stronger pull-off force. At its lowest, the value of the compressibility was close to the value observed for the layered structures.

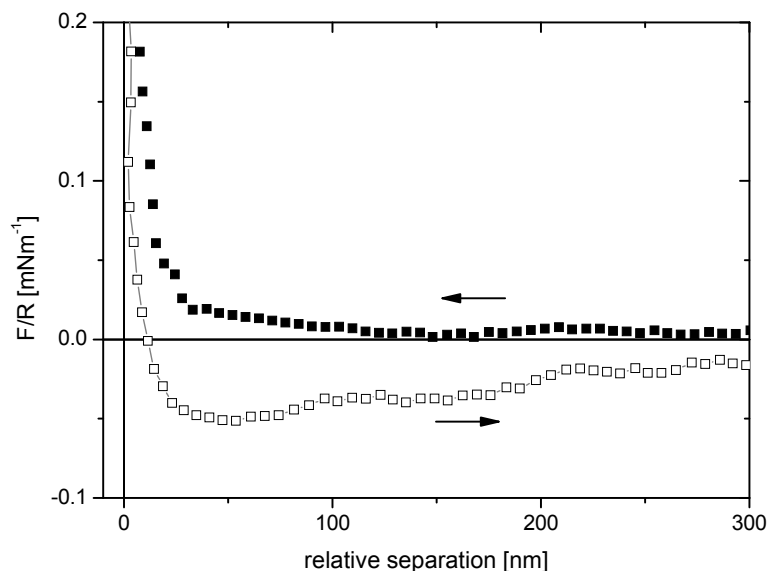


Fig. 10. Pull-off force (open symbols) in 100 mg/l complex of C-PAM and SNP (in mass ratio of 1:1) solution at 11 mM electrolyte concentration. Filled symbols are for approaching data.

DISCUSSION

Multilayer Structures of C-PAM – Silica Nanoparticle

During the multilayer build-up of C-PAM-SNP layers using QCM-D, it was observed that a large amount of SNP was adsorbed on the C-PAM layer (Fig. 1a). Nevertheless, the dissipation was not exceptionally high. In fact, after the addition of the 2nd layer of C-PAM, the dissipation decreased slightly, indicating that the layer became denser. Furthermore, the change in frequency was higher in medium salt concentration. There was a good correlation between the 3rd, 5th, and 7th overtone data, and the Δf of the layers was not dependent on the frequency as with the NFC multilayer system. This might indicate that although the SNP layer had rather high dissipation, it was behaving more uniformly in the depth direction than the NFC layer. AFM images showed a fully covered surface in the multilayer formation of the C-PAM and SNP system. In contrast, when C-PAM and silica nanoparticles were added together as a complex, they only partially covered the surface, revealing the nanofibrillar cellulose structure underneath. Also, the QCM-D results indicated a much smaller adsorbed amount in this case (Fig. 5). RMS roughness and mean Z directional variation were lower for multilayer structure. Clearly, the layered structure was uniform, well-organized, and smooth, whereas the complex structure was more random.

Both multilayer and complex structures were formed of similar granules, which were further organized to larger clusters (Table 2). Granules were size of 80 x 40 nm, and with silica nanoparticles being 25 nm, granules could not contain many nanoparticles. Probably only a part of C-PAM molecules was binding these nanoparticles together,

because the size of a quite similar C-PAM molecule has been observed to be 420 nm (Mabire et al. 1984). The presence of C-PAM is hard to detect with AFM, and thus it was only seen as a binding material. Actually, the clusters formed by the granules are close to the size range of the complexes and C-PAM (Table 1). Considering the changes in conformation due to adsorption, different salt concentration and shrinkage during drying, the complex of C-PAM and SNP can be assumed to have a collapsed pearl necklace structure on surface (Cabane and Duplessix 1982).

During the force measurements repulsion increased all through the multilayer formation, both at low and at medium salt concentration. The repulsion, however, ranged longer at low salt concentration. In addition the addition of SNP had almost no effect on the measured forces at low salt concentration while the increase in repulsion was clear at medium salt concentration. The higher compressibility also indicated a rigid layer in this case.

From the observations above, the uniform layer structure, the high amount of adsorbed SNP, the negligible increase in repulsion upon SNP addition and the similarities in AFM images, it was concluded that silica nanoparticles are able to penetrate inside the loose polyelectrolyte layer due to their small size. A proposed layer structure at medium salt concentration is illustrated in Fig. 11A.

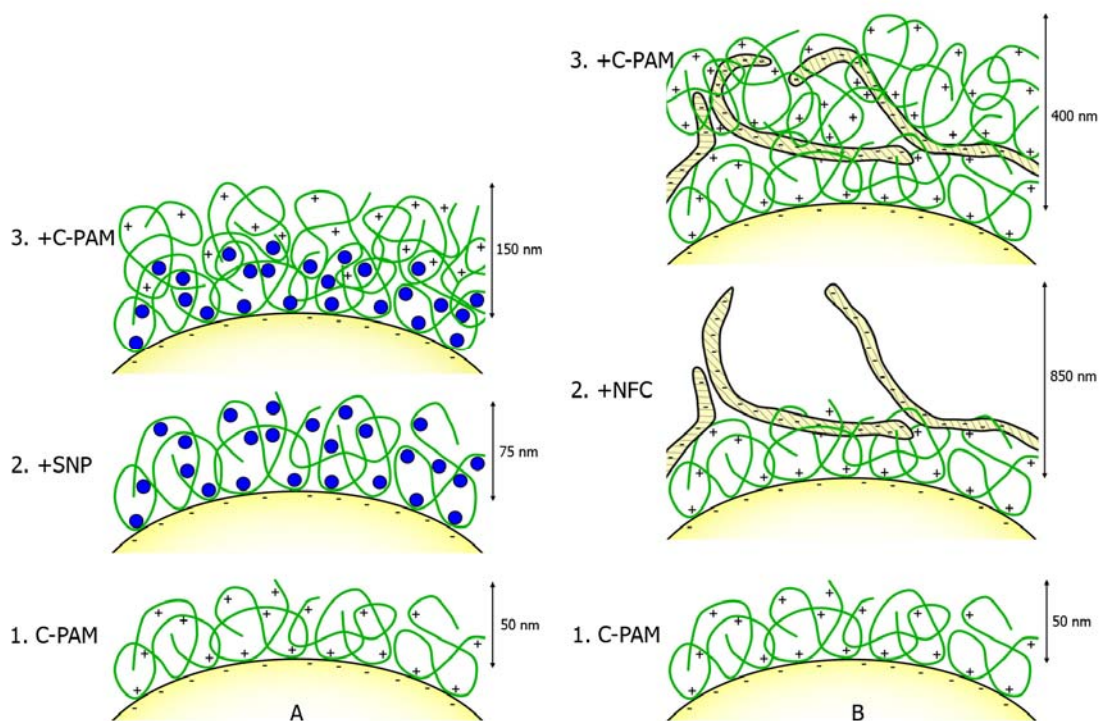


Fig. 11. A schematic image of A. C-PAM-SNP-C-PAM layer and B. C-PAM-NFC-C-PAM layer growth at medium salt concentration. Note that the drawing is not to scale, but indicated scales are given based on the range of repulsion in the force measurements at 11 mM electrolyte solution. The real layer thickness is not known due to uncertainty in zero separation.

At medium salt concentration, the charges of the polyelectrolyte are rather randomly located due to screening of the charges. Hence, the negatively charged nanoparticles are located all over the layer. This leads to strong repulsion between segments, which for its part leads to an increase in layer thickness and repulsion after addition of SNP. At low salt concentration, the charges of polyelectrolyte layer are located only very close to the cellulose surface. Therefore, nanoparticles tend to adsorb near the cellulose surface, where the charges of C-PAM are. This keeps the outermost polymer layer fairly unchanged, which was seen in compressibility value and in the range and magnitude of repulsion. This suggested layer structure could also explain the lack of pull-off force in the medium salt concentration case.

Our formulated model for the nanostructure of the polyelectrolyte-nanoparticle layer deviates from previous models for colloidal particles and polyelectrolyte, in which colloidal particles are suggested to form their own uniform layer (Lvov et al. 1997). This model is often lightly adapted also for nanoparticles. This model may well be true for multilayers between low molecular weight highly charged polyelectrolytes and nanoparticles. However, in our case the C-PAM layer is so loose that the small SNP particles can easily penetrate inside the layer. Such penetration depends on the size of the particle and type of polymer.

Multilayer Structures of C-PAM – Cellulose Nanofibrils

After the initial C-PAM layer, cellulose nanofibrils adsorbed on C-PAM layer formed an extremely loose and viscoelastic layer, in accordance with earlier studies (Ahola et al. 2008a; Aulin et al. 2008). NFC might even form a brushlike structure, as suggested by Ahola et al. (2008a). When C-PAM was added the second time, only a slight change in the dissipation was observed. This, together with the analysis of the overtones, indicated that the structure was stratified, but probably partially overlapping. The polyelectrolyte multilayers have been reported to overlap even by 50% (Decher 1997). In this situation, charges are spread out (Lvov et al. 1993). At this point, the results differ clearly from the observations made with C-PAM-SNP system, where the uniform layer structure was discovered due to the penetration of nanoparticles inside C-PAM layer. C-PAM and NFC formed well-organized layers on cellulose surface (Fig. 1b and 6c). Fibrils did not form aggregates, but they adsorbed as a self-organized network on the C-PAM layer. A similar structure for NFC has been reported by others (Ahola et al. 2008a; Aulin et al. 2008; Wågberg et al. 2008). The multilayer formation is schematically illustrated in Fig. 11B.

The salt concentration affected the C-PAM-NFC multilayer system. The frequency and dissipation increased relatively and the adsorption rate increased with increasing salt concentration. When C-PAM and highly charged NFC form layers on cellulose at medium salt concentration, the interactions were different than during C-PAM and SNP layer formation. First, repulsion increased substantially when nanofibrillar cellulose was added, due to a very thick and loose layer of NFC. Then repulsion decreased clearly in the second addition of C-PAM indicating a slight collapse of the loose layer of nanofibrillar cellulose.

Comparison between Inorganic and Cellulosic Nanoparticles with Respect to some Practical Applications

Initial layers of multilayer structures on high charged mineral surface are affected by the substrate (Buron et al. 2007, Aulin et al. 2008, Wågberg et al. 2008). On the other hand, multilayers of high molecular weight, low charged C-PAM and A-PAM are reported to be unaffected by the surface when comparing silica and cellulose (Saarinen et al. 2008). In our study, we studied only the first three layers, with only cellulose as a substrate; hence, we cannot state how much the substrate affects our results. Nevertheless, the substrate can be used as a tool in multilayer formation, and thus, the effect of substrate should always be considered.

We suggest that the different layer structures obtained when using either SNP or NFC together with C-PAM is mainly due to the difference in the particle size and form. In addition, NFC has a tendency to form networks, and this hinders its penetration into the C-PAM layer. However, the effect of different chemistry cannot be ruled out. Silica nanoparticles are able to penetrate and freely move in a rather loose C-PAM layer, whereas cellulose nanofibrils form a distinct layer. The network of cellulose nanofibrils is able to bind a lot of water and can thus swell considerably. This slows down conformation changes. Quite interestingly, this differs from the behavior observed in case of polyelectrolyte multilayering (Saarinen et al. 2008).

Freely moving, charged silica nanoparticles tend to act as a binding site between charges. Earlier Asselman et al. (2000) and Jiang et al. (2008) suggested that microparticles or nanoparticles act as physical cross-link points between polymer layers. This definitely supports the practical observations that nanoparticles are able to re-flocculate pulp fiber flocs better than dual polymer systems (Andersson and Lindgren 1996; Swerin and Ödberg 1996). Due to their larger size, colloidal particles probably form a separate layer, but they retain the ability to act as a binding site for polymer layers. Furthermore, the addition of SNP and C-PAM as a complex seems to self-regulate adsorption, and to cover the surface only partially. The observed pull-off force indicates that, in this case, flocculation is enhanced by complex bridging. This is different from observations with C-PAM/A-PAM complexes (Salmi et al. 2007b). The layer of C-PAM/A-PAM complex fully covered the surface and still showed pull-off force due to the linking mechanism between layers.

Ahola et al. (2008a) observed that cellulose nanofibrils have a positive effect on paper strength properties both in wet and in dry conditions. Our study supports these observations. Nanofibrillar cellulose definitely forms a loose and open network with long-range interactions and contributes to the amount and quality of fiber-fiber links. NFC is capable of creating nanonetworks inside the macroscopic fiber web. NFC can be utilized as a strengthening agent, but also it may be beneficial for flocculation. Speculatively, if the network of NFC could be adjusted so that it captures fines and fillers, then it can function in the same way as network flocculation (Stenius 2000). However, the NFC layer binds a lot of water, which may lead to trouble in dewatering or in the drying section. This can be eliminated with a proper co-operative polyelectrolyte.

CONCLUSIONS

1. When silica nanoparticles and C-PAM were added sequentially, they formed a uniform and well-ordered layer due to rather freely moving silica nanoparticles inside the polyelectrolyte layer.
2. NFC formed an extremely water-rich layer on C-PAM. In this case the layers did not mix considerably.
3. Overall, QCM-D and AFM results supported each other and provided a good rationalization for observation also on a larger scale, for example, in flocculation and in paper strength experiments.
4. The loose and thick layer of NFC indicated by the large dissipation and long-range repulsion can argue for the benefits of NFC on paper strength.
5. The free movement and binding ability of SNP particles can account for the good reflocculation properties of nanoparticle systems.

ACKNOWLEDGMENTS

The authors thank Dr. Susanna Ahola for valuable discussions regarding cellulose nanofibrils and M.Sc. Delphine Miquel for kindly helping with the preparation of the nanofibrillar cellulose surfaces, when needed. In addition, we thank the technicians Ms. Marja Kärkkäinen and Ms. Ritva Kivelä for the preliminary preparation of the polyelectrolytes and Ms. Anu Anttila for the determination of the solution properties. We are grateful to M.Sc. Mikael Ankerfors (STFI Packforsk) for kindly providing nanofibrils and to Prof. Mark Rutland (KTH) for kindly donating the cellulose spheres. Dr. Joseph Campbell is thanked for the linguistic support. Kemira Oyj is appreciated for providing the polyelectrolytes. This work was funded by The National Technology Agency of Finland (TEKES), Kemira Oyj, UPM-Kymmene and Metso paper through the WoodWisdom-Net project called DesignCell.

REFERENCES CITED

- Ahola, S. (2008). *Properties and interfacial behaviour of cellulose nanofibrils*, Doctoral Thesis, TKK, Espoo, Finland.
- Ahola, S., Österberg, M., and Laine, J. (2008a). "Cellulose nanofibrils – adsorption with poly(amideamine) epichlorohydrin studied by QCM-D and application as a paper strength additive," *Cellulose* 15, 303-314.
- Ahola, S., Salmi, J., Johansson, L.-S., Laine, J., and Österberg, M. (2008). "Model films from native cellulose nanofibrils. preparation, swelling, and surface interactions," *Biomacromolecules* 9, 1273-1282.
- Andersson, K., and Lindgren, E (1996). "Important properties of colloidal silica in microparticulate systems," *Nord. Pulp Pap. Res. J.* 11(1), 15-21.

- Ariga, K., Lvov, Y., Onda, M., Ichinose, I., and Kunitake, T. (1997). "Alternately assembled ultrathin film of silica nanoparticles and linear polycations," *Chem. Lett.* (2), 125-126.
- Asselman, T., Alinec, B., Garnier, G., and Van de Ven, T. G. M. (2000). "Mechanism of polyacrylamide-bentonite microparticulate retention aids," *Nord. Pulp Paper Res. J.* 15(5), 515-519.
- Aulin, C., Varga, I., Claesson, P.M., Wågberg, L., and Lindström, T. (2008). "Build-up of polyelectrolyte multilayers of polyethyleneimine and microfibrillated cellulose studied by in situ dual-polarization interferometry and quartz crystal microbalance with dissipation," *Langmuir* 24(6), 2509-2518.
- Aulin, C., Ahola, S., Josefsson, P., Nishino, T., Hirose, Y., Österberg, M., and Wågberg, L. (2009). "Nanoscale cellulose films with different crystallinity – Their surface properties and interaction with water," *Langmuir*, submitted.
- Berglund, L. (2005). "Cellulose -based nanocomposites," *Natural Fibers, Biopolymers, and Biocomposites*, 807-832.
- Bergström, L., Stemme, S., Dahlfors, T., Arwin, H., and Ödberg, L. (1999). "Spectroscopic ellipsometry characterization and estimation of the Hamaker constant of cellulose," *Cellulose* 6(1), 1-13.
- Bogdanovic, G., Sennerfors, T., Zhmud, B., and Tiberg, F. (2002). "Formation and structure of polyelectrolyte and nanoparticle multilayers: Effect of particle characteristics," *J. Colloid Interface Sci.* 255(1), 44-51.
- Buron, C.C., Filiatre, C., Membrey, F., Bainier, C., Charrat, D., and Foissy, A. (2007). "Early steps in layer-by-layer construction of polyelectrolyte films: The transition from surface/polymer to polymer/polymer determining interactions," *J. Colloid Interface Sci.* 314(2), 358-366.
- Butt, H.-J. (1991). "Measuring electrostatic, van der Waals, and hydration forces in electrolyte solutions with an atomic force microscope," *Biophys. J.* 60(6), 1438-1444.
- Cabane, B., and Duplessix, R. (1982). "Organization of surfactant micelles adsorbed on a polymer molecule in water: a neutron scattering study," *Journal de Physique (Paris)* 43(10), 1529-1542.
- Carambassis, A., and Rutland, M. W. (1999). "Interactions of cellulose surfaces: Effect of electrolyte," *Langmuir* 15(17), 5584-5590.
- Decher, G. (1997). "Fuzzy nanoassemblies: Toward layered polymeric multicomposites," *Science* 277(5330), 1232-1237.
- Decher, G., Hong, J. D., and Schmitt J. (1992). "Buildup of ultrathin multilayer films by a self-assembly process: III. Consecutively alternating adsorption of anionic and cationic polyelectrolytes on charged surfaces," *Thin solid films* 210-211, 831-835.
- Derjaguin, B. (1934). "Untersuchungen über die Reibung und Adhäsion," *Kolloid-Zeit.* 69, 155.
- Derjaguin, B. V., Churaev, N. V., and Muller, V. M. (1987). *Surface Forces*, Consultants Bureau, New York.
- Donnan, F. G. (1912). "The theory of membrane equilibrium in the presence of a non-dialyzable electrolyte," *Z. Elektrochem.* 17, 572.
- Ducker, W., Senden, T., and Pashley, R. (1991). "Direct measurement of colloidal forces using an atomic force microscope," *Nature* 353(6341), 239-241.

- Holmberg, M., Berg, J., Stemme, S., Ödberg, L., Rasmusson, J., and Claesson, P. (1997). "Surface force studies of Langmuir-Blodgett cellulose films," *J. Colloid Interface Sci.* 186(2), 369-381.
- Hubbe, M. A., Rojas, O. J., Lucia, L. A., and Sain, M. (2008). "Cellulosic nanocomposites: A review," *BioRes.* 3(3), 929-980.
- Hutter, J. L., and Bechhöfer, J. (1993). "Calibration of atomic-force microscope tips," *Rev. Sci. Instrum.* 64(7), 1868-1873.
- Jiang, A., Shen, Y., and Wu, P. (2008). "Self-assembly of multilayer films containing gold nanoparticles via hydrogen bonding," *J. Colloid Interface Sci.* 319, 398-405.
- Kotov, N. A., Dekany, I., and Fendler, J. H. (1995). "Layer-by-layer self-assembly of polyelectrolyte-semiconductor nanoparticle composite films," *J. Phys. Chem.* 99(35), 13065-13069.
- Lvov, Y., Decher, G., and Moehwald, H. (1993). "Assembly, structural characterization, and thermal behavior of layer-by-layer deposited ultrathin films of poly(vinyl sulfate) and poly(allylamine)," *Langmuir* 9(2), 481-486.
- Lvov, Y., Ariga, K., Onda, M., Ichinose, I., and Kunitake, T. (1997). "Alternate Assembly of Ordered Multilayers of SiO₂ and Other Nanoparticles and Polyions," *Langmuir* 13(23), 6195-6203.
- Mabire, F., Audebert, R., and Quivoron, C. (1984). "Synthesis and solution properties of water soluble copolymers based on acrylamide and quaternary ammonium acrylic comonomer," *Polymer* 25(9), 1317-1322.
- Paananen, A., Österberg, M., Rutland, M., Tammelin, T., Saarinen, T., Tappura, K., and Stenius, P. (2004). "Interaction between cellulose and xylan: An atomic force microscope and quartz crystal microbalance study," *ACS Symp. Ser.* 864, 269-290.
- Pääkkö, M., Ankerfors, M., Kosonen, H., Nykänen, A., Ahola, S., Österberg, M., Ruokolainen, J., Laine, J., Larsson, P.T., Ikkala, O., and Lindström, T. (2007). "Enzymatic hydrolysis combined with mechanical shearing and high-pressure homogenization for nanoscale cellulose fibrils and strong gels," *Biomacromolecules* 8(6), 1934-1941.
- Procter, H. R., and Wilson, J. A. (1916). "The acid-gelatin equilibria," *J. Chem. Soc.* 109, 1307-1319.
- Rutland, M. W., Tyrrell, J.W.G., and Attard, P. (2004). "Analysis of atomic force microscopy data for deformable materials," *J. Adhesion Sci. Technol.* 18(10), 1199-1215.
- Saarinen, T., Österberg, M., and Laine, J. (2008). "Adsorption of polyelectrolyte multilayers and complexes on silica and cellulose surfaces studied by QCM-D," *Colloids Surf. A* 330(2-3), 134-142.
- Salmi, J., Österberg, M., Stenius, P., and Laine, J. (2007a). "Surface forces between cellulose surfaces in cationic polyelectrolyte solutions: The effect of polymer molecular weight and charge density," *Nord. Pulp Pap. Res. J.* 22(2), 249-257.
- Salmi, J., Österberg, M., and Laine, J. (2007b). "The effect of cationic polyelectrolyte complexes on interactions between cellulose surfaces," *Colloids Surf. A* 297(1-3), 122-130.

- Sennerfors, T., Fröberg, J. C., and Tiberg, F. (2000). "Adsorption of polyelectrolyte-nanoparticle systems on silica: Influence on interaction forces," *J. Colloid Interface Sci.* 228(1), 127-134.
- Stenius, P. (2000). "Macromolecular, surface and colloid chemistry," In *Forest Products Chemistry*, Stenius, P. (ed), Fapet OY, Helsinki, Finland.
- Stiernstedt, J., Brumer, H. III, Zhou, Q., Teeri, T. T., and Rutland, M. W. (2006). "Friction between cellulose surfaces and the effect of and xyloglucan adsorption," *Biomacromolecules* 7(7), 2147-2153.
- Swerin, A., and Ödberg, L. (1996). "Flocculation of cellulosic fiber suspensions by a microparticulate retention aid system consisting of cationic polyacrylamide and anionic montmorillonite. Effect of contact time, shear level and electrolyte concentration," *Nord. Pulp Paper Res. J.* 11(1), 22-29.
- Torii, A., Sasaki, M., Hane, K., and Okuma, S. (1996). "A method for determining the spring constant of cantilevers for atomic force microscopy," *Meas. Sci. Technol.* 7(2), 179-184.
- Tortonese, M., and Kirk, M. (1997). "Characterization of application specific probes for SPMs," *Proceedings of SPIE - The International Society for Optical Engineering* 3009(Micromachining and Imaging), 53-60.
- Wågberg, L., and Lindström, T. (1987). "Some fundamental aspects on dual component retention aid systems," *Nord. Pulp Pap. Res. J.* 2(2), 49-55.
- Wågberg, L., Decher, G., Norgren, M., Lindström, T., Ankerfors, M., and Axnäs, K. (2008). "The build-up of polyelectrolyte multilayers of microfibrillated cellulose and cationic polyelectrolytes," *Langmuir* 24(3), 784-795.
- Zauscher, S., and Klingenberg, D. J. (2000). "Normal forces between cellulose surfaces measured with colloidal probe microscopy," *J. Colloid Interface Sci.* 229(2), 497-510.
- Zimmermann, T., Bordeanu, N., Eyholzer, C., and Richter, K. (2008). "High potential of cellulose nanofibrils for technical applications," *Abstracts of Papers*, 235th ACS National Meeting, New Orleans, LA, United States, April 6-10.

Article submitted: Feb. 25, 2009; Peer review completed: March 23, 2009; Revised version received and accepted: March 15, 2009; Published March 16, 2009.